2018-08-15

Herpes ICP8 protein stimulates homologous recombination in human cells

Melvys Valledor
University of Massachusetts Medical School

Et al.

PLOS ONE

RESEARCH ARTICLE

Herpes ICP8 protein stimulates homologous recombination in human cells

Melvys Valledor[1], Richard S. Myers[2]*, Paul C. Schiller[3,4]

1 Department of Neurology, University of Massachusetts Medical School, Worcester, Massachusetts, United States of America, **2** Department of Biochemistry and Molecular Biology, University of Miami Miller School of Medicine, Miami, Florida, United States of America, **3** Department of Orthopaedics, University of Miami Miller School of Medicine, Miami, Florida, United States of America, **4** Geriatric Research, Education, and Clinical Center and Research Service, Bruce W. Carter VAMC, Miami, Florida, United States of America

* rmyers@med.miami.edu

Citation: Valledor M, Myers RS, Schiller PC (2018) Herpes ICP8 protein stimulates homologous recombination in human cells. PLoS ONE 13(8): e0200955. https://doi.org/10.1371/journal.pone.0200955

Editor: Alvaro Galli, CNR, ITALY

Received: March 6, 2018

Accepted: July 4, 2018

Published: August 15, 2018

Data Availability Statement: All relevant data are within the paper and its Supporting Information files.

Funding: This work was supported by the National Institutes of Health [F31-GM089125-01] to MV, funds from the University of Miami Department of Biochemistry and Molecular Biology to RSM, Department of Veterans Affairs, Veterans Health Administration, Office of Research and Development (Biomedical Laboratory Research and Development) Merit Review award [BX000952] to PCS and funds from the Miami VA Geriatric Research, Education, and Clinical Center

Abstract

Recombineering has transformed functional genomic analysis. Genome modification by recombineering using the phage lambda Red homologous recombination protein Beta in *Escherichia coli* has approached 100% efficiency. While highly efficient in *E. coli*, recombineering using the Red Synaptase/Exonuclease pair (SynExo) in other organisms declines in efficiency roughly correlating with phylogenetic distance from *E. coli*. SynExo recombinases are common to double-stranded DNA viruses infecting a variety of organisms, including humans. Human Herpes virus 1 (HHV1) encodes a SynExo comprised of ICP8 synaptase and UL12 exonuclease. In a previous study, the Herpes SynExo was reconstituted *in vitro* and shown to catalyze a model recombination reaction. Here we describe stimulation of gene targeting to edit a novel fluorescent protein gene in the human genome using ICP8 and compared its efficiency to that of a "humanized" version of Beta protein from phage λ. ICP8 significantly enhanced gene targeting rates in HEK 293T cells while Beta was not only unable to catalyze recombineering but inhibited gene targeting using endogenous recombination functions, despite both synaptases being well-expressed and localized to the nucleus. This proof of concept encourages developing species-specific SynExo recombinases for genome engineering.

Introduction

Bacterial recombineering is a widely employed method that catalyzes highly efficient homologous recombination using viral two-component recombination modules referred to as SynExo complexes [1]. The exonuclease component of the SynExo resects linear dsDNA substrates to create single-stranded DNA (ssDNA) ends. The synaptase component of the SynExo is loaded onto the nascent ssDNA to form a protein-DNA filament that catalyzes the search for homology and subsequent annealing to the homologous DNA target. The annealed recombination intermediate can prime DNA synthesis using the 3' end of the invading ssDNA and the paired template DNA. Ultimately, the invading ssDNA becomes covalently joined to the targeted DNA and stably transmitted as a permanent part of the target DNA. Recombineering has

to PCS and MV. The funders had no role in study design, data collection and analysis, decision to publish, or preparation of the manuscript.

Competing interests: The authors have declared that no competing interests exist.

become instrumental in analyzing gene function in bacteria since genome modification can be seamless and is both specific and highly efficient, especially when one simplifies the reaction by using ssDNA oligonucleotides (ssDNA oligos) as substrates and the synaptase component of the SynExo [2, 3]. A model for ssDNA recombineering is illustrated in Fig 1.

Eukaryotic genome segments have been recombineered with high efficiency in bacteria, but not yet in eukaryotic cells. Efforts to move enterobacteria phage SynExos into other organisms have had mixed success, depending on the phylogenetic distance from *E. coli*. For example, *Shigella* and *Salmonella* genomes have been successfully engineered using the λ Red SynExo to perform epitope tag insertion, deletions and site-directed mutagenesis [4], but recombineering efforts using enterobacteria phage SynExos in organisms more distantly related to *E. coli* have met less success [5, 6]. Very low efficiency genomic ssDNA recombineering has also been reported in mouse embryonic stem cells using Beta protein from bacteriophage lambda [7], although it was not clear from the reported data how well Beta was expressed and whether Beta was properly localized to the nucleus in the mouse cells. However, the negative correlation of phylogenetic distance between the host origin of the viral SynExo and the target organism with the efficiency of recombineering suggests that it may be necessary to maintain interactions between coevolved viral SynExo proteins and unknown host factors for efficient recombination.

SynExo recombinase genes appear to be common to genomes of double strand DNA (dsDNA) viruses with no RNA stage [8, 9]. Putative SynExo components have been found in viruses that infect most types of bacteria, some archae, and many eukaryotes (S1 Fig). Efforts to develop alternative SynExos (*e.g.* S1 Table) that are "evolutionarily tuned" to engineer specific genomes have yielded encouraging results [10, 11, 12]. We propose that in order to extend the power of recombineering to human cells, a human viral SynExo should be employed. We previously identified a SynExo in human Herpes virus 1 (HHV1) comprised of ICP8 synaptase + UL12 exonuclease [8] and subsequently showed [13] that the HHV1 SynExo catalyzes strand exchange in an *in vitro* model of recombination using dsDNA. More recently, the HHV1 SynExo was reported to stimulate dsDNA break repair in rad52-deficient human 293 cells [14].

Since ssDNA recombineering is more efficient in bacteria and only requires the synaptase component of the SynExo complex, we tested ssDNA recombineering in human cells using the well-characterized bacteriophage synaptase Beta and the human viral synaptase ICP8. We predicted that if recombineering were host-specific, a human viral synaptase would more efficiently promote gene targeting in human cells than would the enterobacteria phage synaptase Beta. Here we evaluated ssDNA recombineering in human cells in the presence of either the human viral synaptase ICP8 or the bacteriophage synaptase Beta.

Results

Creation of fluorescent human recombineering reporter cell lines

For this proof of concept, we created a quantitative and sensitive reporter for genome editing using ssDNA oligos. To avoid false positives from sporadic mutations that either activate or inactivate a gene, we choose to change the emission spectrum of eGFP by targeting codon 203 (threonine, T) to code for another amino acid (tyrosine, Y) to yield a red-shifted fluorescent protein (referred to as Mostaza in [15] and Yellow in this report) (Fig 2 panels A and B). Lentiviral vectors based on pDual-eGFP [15] were created to transduce human 293T cells with lentiviruses carrying eGFP or eGFPT203Y. Green (eGFP) and Yellow (eGFPT203Y) expressing cells could be distinguished and quantified by flow cytometry (Fig 2 panels C-E), which allowed us to evaluate a large number of cells in each trial (Fig 2 panel F). The recombineering assay used oligo substrates that introduce 4 nucleotide substitutions and change the Yellow cell

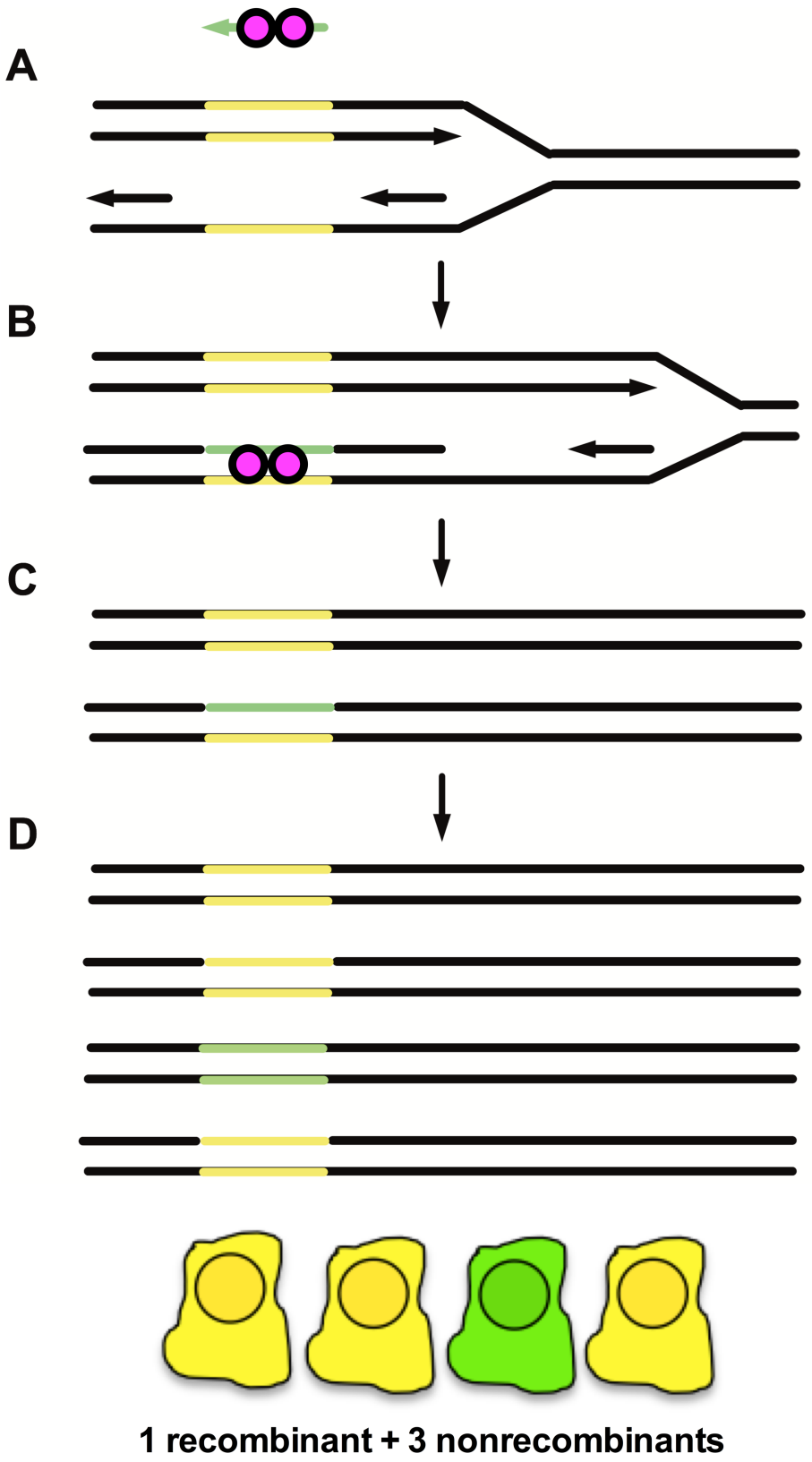

Fig 1. ssDNA (oligo) recombineering model. A) Synaptases (pink balls) bind to ssDNA (represented by the green left-facing arrow at top) to form a nucleoprotein filament. B) The nucleoprotein filament samples ssDNA sequences

between Okazaki fragments in replicating DNA. Synaptases promote annealing of the nucleoprotein filament to complementary ssDNA. C) The ssDNA oligo becomes joined to replicating DNA between Okazaki fragments. Completion of replication yields one nonrecombinant chromosome and one recombinant heteroduplex chromosome. D) A second round of replication and division yields one fully recombinant cell (green) and 3 nonrecombinant cells (yellow) from a cell bearing one initially recombinant target chromosome.

https://doi.org/10.1371/journal.pone.0200955.g001

fluorescence to Green (Fig 2 panel A and S2 Fig). While the change from green to yellow and vice verse could be accomplished with a two nucleotide substitution, the addition of 2 additional silent substitutions created a bubble when the oligo anneals the template predicted to better evade DNA mismatch repair (MMR) (S2 Fig panel B) [15]. Incorporation of these silent mutations also allowed us to distinguish real recombinants from revertants or eGFP contamination.

Sources of viral synaptases in reporter cell line 293T-Yellow: ICP8 and HumBeta

This study aimed to evaluate if viral synaptases can promote gene targeting in human cells. While Beta protein is very efficient in bacteria, we predicted that an analogous ssDNA annealing protein (ICP8) from a human herpes virus would be more efficient for recombineering in human cells. In these studies ICP8 was transiently expressed from plasmid pCMV-ICP8 and from a stably integrated inducible system. We noticed cell death after pCMV-ICP8 transfection, which reduced recovery of recombinant progeny (data not shown). However, viable recombinants remained

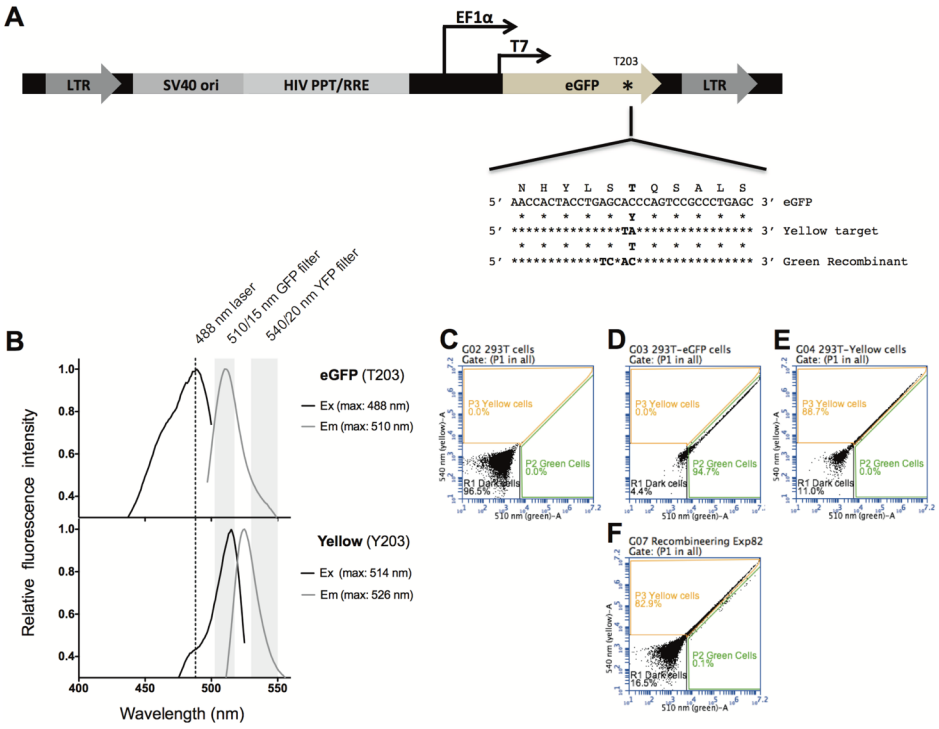

Fig 2. Fluorescent recombineering reporter. A) Lentiviral vector pDual-eGFP^{Y203} was used to deliver a Yellow florescent protein variant of eGFP to serve as the recombineering target transgene. B) Fluorescence excitation and emission spectra of purified eGFP and eGFP^{Y203} proteins. C-F) Flow cytometry was used to quantify 293T-Green recombinant and 293T-Yellow parental phenotypes. C) Untransduced cells were quantified in the R1 gate, D) pDual-eGFP transduced Green cells were quantified in the P2 gate and E) pDual-eGFP ^{Y203} transduced Yellow cells were quantified in the P3 gate. F) Example results from one recombination experiment using Yellow cells as a target and an oligo that codes for Green fluorescence.

https://doi.org/10.1371/journal.pone.0200955.g002

present after 9 nine days of outgrowth, suggesting that more controlled delivery of ICP8 function might improve outcomes. Furthermore, variable pCMV-ICP8 transfection efficiencies contributed to varying apparent recombineering rates. Therefore, we created stable cell lines that expressed ICP8 under the control of a doxycycline-inducible (Dox) promoter. In parallel, we created similar cell lines expressing the *E. coli* bacteriophage synaptase Beta under control of Dox. To ensure that the bacteriophage synaptase Beta would be expressed in human cells, the coding sequence was optimized for translation in mammalian cells and a nuclear localization signal was added to direct Beta to the nucleus. We called this synthetic protein "HumBeta". In this way, we attempted to mimic an efficient bacterial recombineering protocol [15] where the synaptases are expressed from stable transgenes in a burst of induction just before adding the oligo substrate for recombination. By comparing recombineering efficiency using a synaptase from a virus that co-evolved with humans and a synaptase that co-evolved with a bacterium, we surmised we might probe host specificity of recombineering.

Synaptase genes were co-expressed with a red fluorescent protein gene, E2-Crimson [16], in a polycistronic system using a P2A linker. The P2A linker causes ribosome skipping to independently produce equimolar amounts of the upstream and downstream protein products [17] with a few amino acids added to each protein product. Since a GFP-ICP8 and Beta-SPA Fusions reduced each protein's activity [18, 19], both synaptases were cloned 5' and 3' of the Crimson reporter in pSLIK vectors. Six pSLIK/TREPitt lentiviral plasmid constructions were created by cloning the synaptase genes either 5' or 3' to E2-Crimson in separate lentiviral constructs (S3 Fig; details of plasmid and cell line construction are presented in S1 Extended Methods). Lentivirus particles produced from these lentiviral vectors were used to transduce 293T-Yellow cells. Synaptase expression was inferred from E2-Crimson fluorescence (S4 Fig) and confirmed by Western Blot (S5 Fig) and immunostaining (S4 Fig). Following induction of expression by doxycycline, ICP8 and HumBeta localized to the nucleus (S4 Fig). ICP8 was either evenly distributed or formed bright punctuate dots, similar to those described in a previous report [20], albeit in the absence of other HHV1 proteins. Unlike ICP8, HumBeta did not organize into punctuate subnuclear dots but was evenly distributed throughout the nucleus (S4 Fig), occasionally accumulating at the nuclear periphery (not shown).

HHV1 ICP8 protein stimulates gene targeting in human cells

Gene targeting was evaluated in 293T-Yellow cells expressing ICP8 either from transiently transfected pCMV-ICP8 or from stably transduced pSLIK 1 & 4. Recombinant cells were identified by a shift in fluorescence from Yellow to Green using flow cytometry (Fig 2 panel F). The average frequency of Green fluorescent cells among total fluorescent cells after subtracting the background from the no-oligo controls in 8 independent experiments was close to 0.2% while endogenous rates were below 0.1% (data from Figs 3–6 and S6). In Fig 3 panel B, human Herpes ICP8 stimulates gene targeting over endogenous recombination functions by 2.3-fold. We likely underestimated the amount of recombination promoted by ICP8 in these experiments, as it became evident that not all the cells responded to doxycycline induction. Since Crimson is expressed in equimolar amount to the synaptase, via translational coupling through a P2A linker, recombineering efficiency was measured in the subpopulation of cells expressing Crimson (Fig 3 panels C-D). If recombination is measured in ICP8-expressing cells only, then gene targeting was stimulated 4.7-fold over endogenous rates.

Humanized Beta protein inhibits gene targeting in human cells

In parallel trials to those with ICP8, recombineering was evaluated in cells stably transduced with the humanized bacteriophage HumBeta synaptase. As in experiments with ICP8,

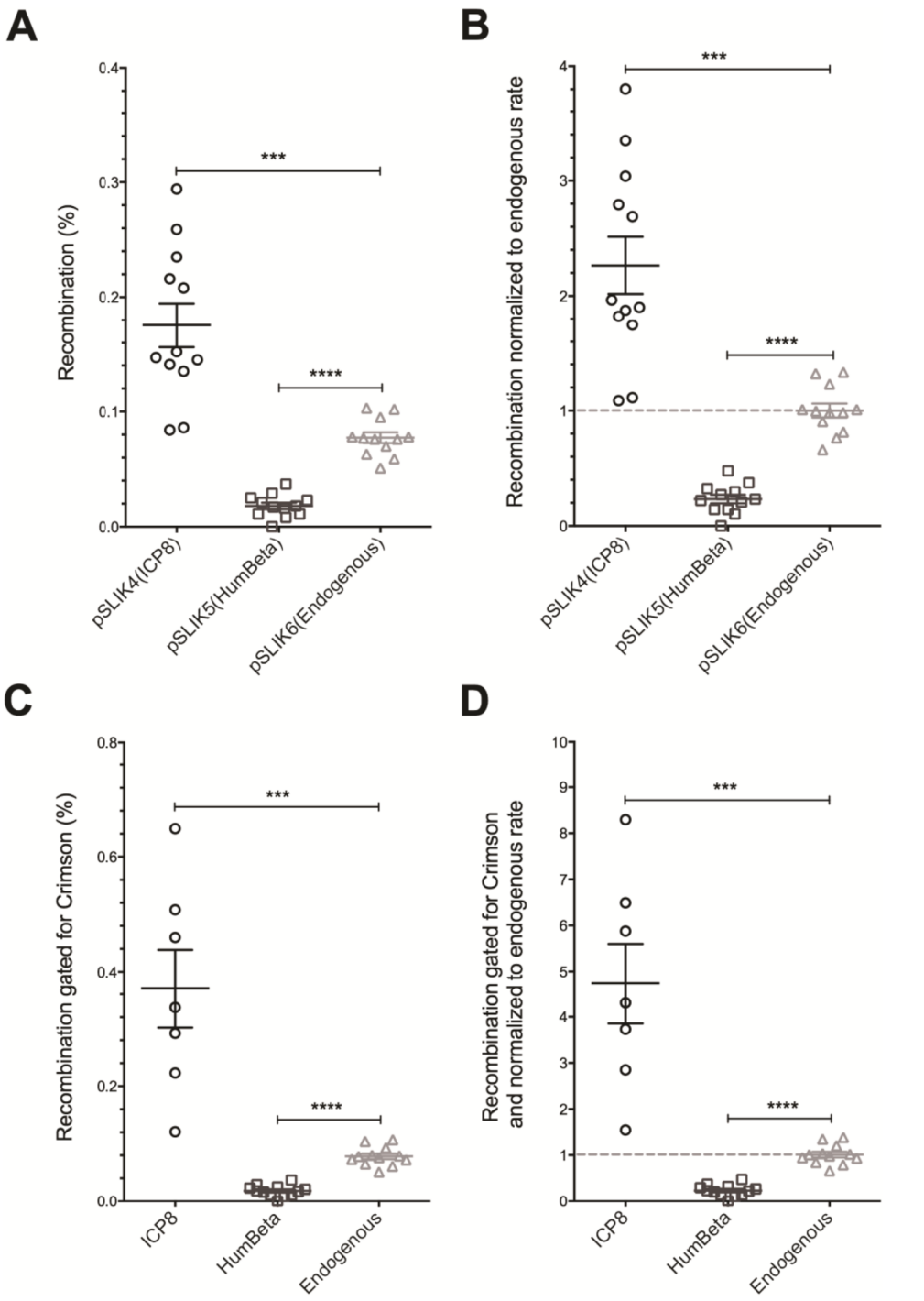

Fig 3. Gene targeting is stimulated by HHV1 ICP8 and inhibited by phage λ Beta in human cells. Cells were incubated with doxycycline to induce synaptase expression and subsequently transfected with 50 nM of oligo 85. A) The background of green cells in "no oligo" control experiments (0.001% for pSLIK4, 0.003% for pSLIK5 and 0.012% for pSLIK6) was subtracted from recombination frequencies. B) Recombination frequencies in (A) were normalized to the mean of the endogenous recombination frequencies in the pSLIK6 control line. C) Cells were gated for Crimson expression (which is expressed in equimolar amounts with the synaptase via translational coupling through a P2A linker) and evaluated as in (A). D) Recombination frequencies in (C) were normalized to the mean of the endogenous recombination frequencies in the pSLIK6 control line and evaluated as in (A). Data were evaluated by Fisher's Exact Test of significance; *** indicates $P<0.005$ and **** indicates $P<0.001$. The figure shows sample data from one of eight biological replicates, n = 12 trials, and error bars reflect SEM.

https://doi.org/10.1371/journal.pone.0200955.g003

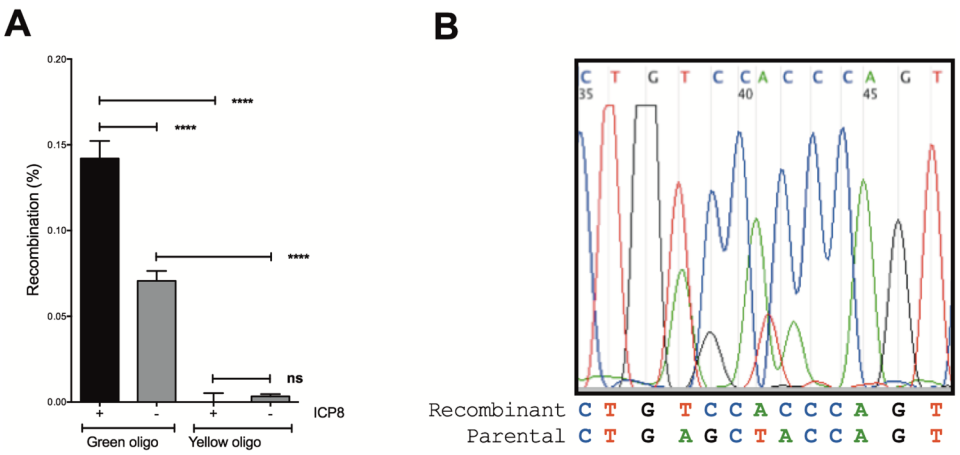

Fig 4. Transfer of the oligo sequence to the genome is required to change cell fluorescence. A) The Green recombinant phenotype requires a Green oligo substrate. Yellow to Green phenotypic conversion was evaluated by transient transfection with pCMV-ICP8 followed by transfection with 200 nM Green or Yellow oligos (85 and 131 respectively). B) Recombinant cells acquire the oligo sequence. A recombinant cell mixture was sorted for Green fluorescent cells. Genomic DNA was isolated from sorted cells enriched for putative recombinants. The target region was amplified by PCR and the products treated with restriction enzyme AluI to cut non-recombinant sequences. Uncut fragments were gel extracted and sequenced using primer 216. The original Parental sequence and the predicted Recombinant sequence is shown. Details of this experiment can be found in S1 Extended Methods under Determination of recombinant genotype.

https://doi.org/10.1371/journal.pone.0200955.g004

HumBeta was induced by doxycycline and cells were subsequently transfected with oligos to assess recombination rates. The average frequency of Green fluorescent cells among total fluorescent cells after subtracting the background from the no-oligo controls was 0.02% for HumBeta cell lines produced by transduction with pSLIK2 or pSLIK5 (Figs 3 and S6). HumBeta cell lines were almost 100% Crimson positive (pSLIK5 gated for Crimson vs pSLIK6, n = 12, P = 1), therefore gating cells for Crimson expression did not modify the initial estimate of recombineering efficiency (Fig 3 panels C-D). In striking contrast to ICP8, expression of HumBeta *inhibited* endogenous rates of gene targeting by 4.3-fold. Inhibition of endogenous recombination may result from sequestration of the oligo into non-productive Beta/DNA complexes, perhaps due to lack of host-specific protein interactions (see discussion). The observation that 100% of the cells with HumBeta were Crimson positive suggests that HumBeta transgene expression was not toxic to cells.

Confirmation of authentic gene targeting by ICP8

To determine if Green fluorescence in putative recombinants was due to inheriting the oligo sequence and not from alternative events, gene targeting experiments were also performed with a Yellow "selfing" oligo with the same sequence as the target (Figs S2 and 4 panel A). The Yellow selfing oligo did not stimulate Green cell formation in either the presence (P = 0.54) or absence (P = 0.41) of ICP8. This is to be expected if transfection of oligos in the presence of ICP8 does not stimulate Yellow to Green conversion via general mutagenesis or green autofluorescence. In this experiment, ICP8 expression increased the frequency of producing Green recombinants 2-fold above endogenous recombination ($P = 7.1x10^{-6}$ by Fisher's Exact Test) when the Green oligo was used.

Evidence that the Green allele sequence was transferred from the recombineering oligo to the genome in cells expressing ICP8 was obtained by allele-specific PCR (S7 Fig). Putative recombinant Green cells were enriched from non-recombinant Yellow cells by cell sorting.

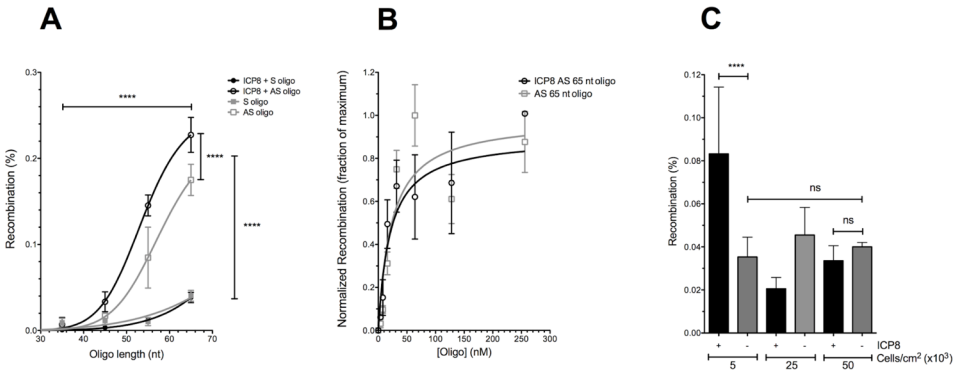

Fig 5. Optimization of human cell recombineering. During the course of developing this platform for human cell recombineering by ICP8, the frequency of gene targeting varied by 10 to 20 fold, influenced by the design and concentration of the oligo substrate, as well as the cell density in the well during oligo transfection. A) **ICP8 and endogenous recombination was significantly improved by longer and antisense oligos**. 293T-Yellow cells were sequentially transfected with pCMV-ICP8 and with oligos that donate the sequence for converting Yellow to Green fluorescence. Recombination was measured as a function of oligo size and the targeted strand. AS oligo indicates that the oligo corresponds to the antisense strand of $eGFP^{Y203}$ and S oligo indicates that the oligo corresponds to the sense strand of $eGFP^{Y203}$. The no oligo background for 293T or 293T-pCMV-ICP8 was subtracted from each data point and never exceeded 0.004%. Fisher's Exact Test was used to evaluate statistical significance with **** indicating $P<0.001$; n = 3. Recombination rates as a function of oligo length could be fit to a one site binding equation (site size 10 nucleotides) with a Hill slope parameter based on previous knowledge of the cooperativity of ICP8 binding to DNA [26]. B) **Recombination rates improved as a function of oligo concentration.** The effect of oligo concentration on gene targeting was evaluated from 4 to 256 nM. Recombination with oligo 85 was measured in pSLIK4 and pSLIK6 cell lines induced with 1 μg/ml doxycycline as a function of oligo concentration. Recombinants were quantified by flow cytometry, normalized to the maximum value for each cell line and fit to a one site binding equation (site size 10 nucleotides) that accounts for depletion of free recombination proteins at saturating oligo concentration. C) **ICP8 requires replicating cells.** In the course of these studies, it became evident that some of the fluctuation in recombination rates observed was due to differences in the density of cells plated before addition of oligos. Recombination with 50 nM antisense oligo 85 was measured in pSLIK4 and pSLIK6 cell lines induced with 1 μg/ml doxycycline and plated at densities of 5000, 25000 and 50000 cells per cm2. Recombinants were quantified by flow cytometry. Fisher's Exact Test was used to evaluate statistical significance with **** indicating $P<0.001$ and ns indicating $P>0.05$; n = 3.

https://doi.org/10.1371/journal.pone.0200955.g005

Sequence results are expected to be a mixture of Green and Yellow sequence, since green cells are expected to have at least one recombinant target copy, but might also have additional non-recombinant target copies due to multiple insertions of the fluorescent transgene. In addition, since ssDNA recombineering targets only one strand of replicating DNA, cells need to go through two cell divisions to segregate the recombinant from non-recombinant targets in a clone (Fig 1). We saw that the recombinant Green cells produced more products when amplified with a primer specific for the Green allele than with a primer specific to the Yellow allele. These results suggest that Green cells incorporated the Green oligo sequence via recombination.

Gene editing was confirmed by DNA sequencing of PCR products amplified from recombinant Green cells. The results shown in Fig 4 panel B, indicate that the sequence from the Green allele (TCCAC) is more prominent than the sequence of the Yellow allele (AGCTA) in Green cells. The silent mutations introduced to abrogate MMR were transferred along with the mutations that converted Yellow to Green, suggesting that Green cells did not arise by reversion or contamination. Taken together, it is evident that *bona fide* ICP8-dependent recombineering is modifying human genomic DNA at the target region as specified by the oligo sequence.

Oligo substrates

In bacterial recombineering, the most efficient substrates are ssDNA oligos in the range of 60 to 100 nt long [21], similar to oligo lengths commonly used for gene targeting in mammalian cells

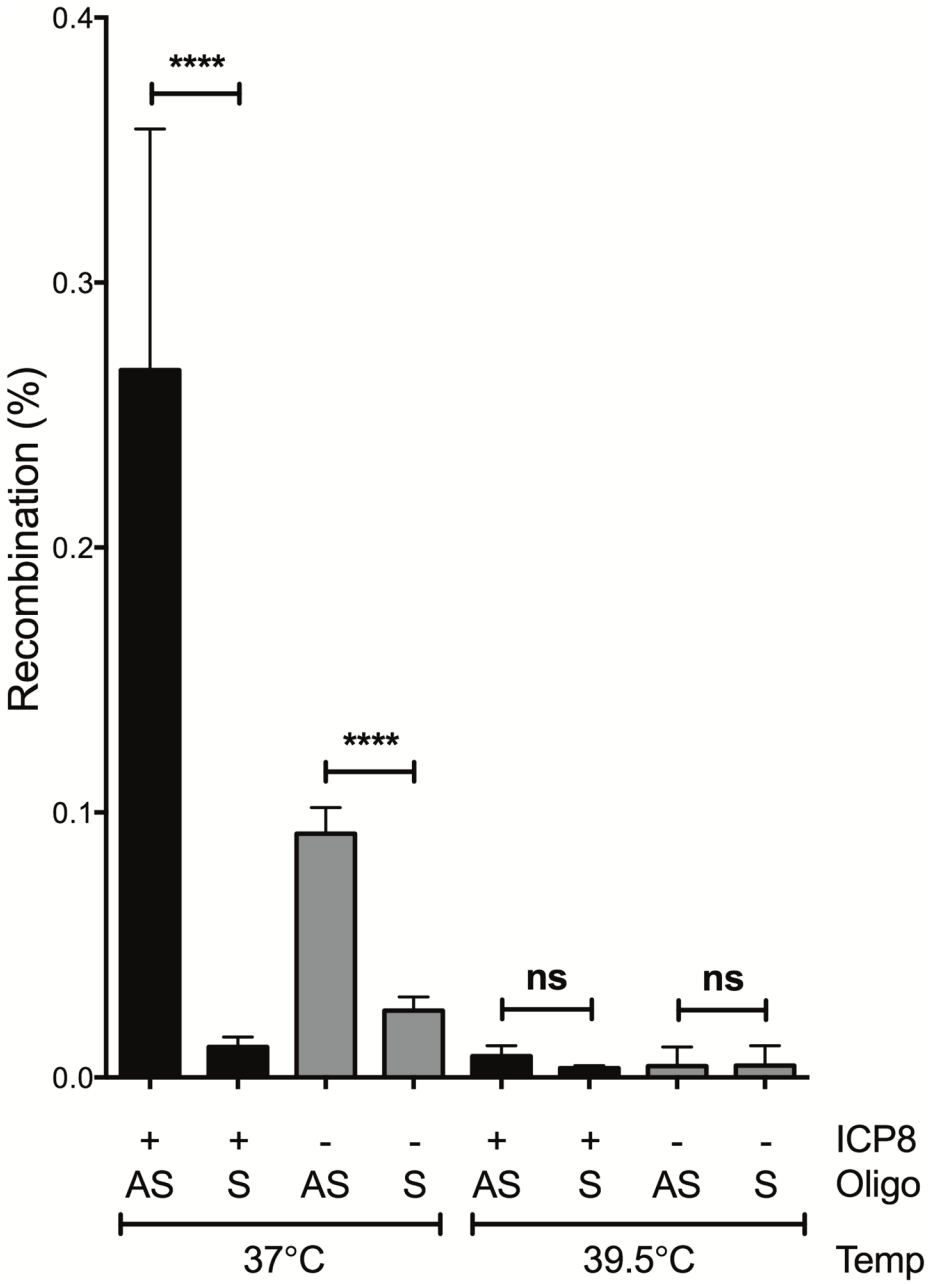

Fig 6. Recombineering strand bias depends on replication originating from the SV40 origin in the integrated lentiviral transgenic target. Recombination was measured in pSLIK4 and pSLIK6 lines using antisense or sense oligos. Cells were grown either at 37˚C (T antigen active), or at 39.5˚C (T antigen does not bind to or promote replication from the SV40 origin). Fisher's Exact Test was used to evaluate statistical significance with **** indicating $P<0.001$ and ns indicating $P>0.05$. n = 3.

https://doi.org/10.1371/journal.pone.0200955.g006

[22, 23]. Shorter oligos (20–25 nt) require modification to be effective as the introduced sequences are more susceptible to exonucleases [23, 24]. To avoid potential DNA damage induced by modified DNA [25], unmodified oligos of varying lengths were tested (Fig 5 panel A). Recombination rates improved as a function of oligo length and could be fit to a one-site binding equation with a Hill slope parameter based on previous knowledge of the cooperativity

of ICP8 binding to DNA [26]. Recombination was significantly improved as oligo length increased (by Fisher's Exact Test) in pairwise comparisons of each DNA length for a given oligo sequence in each cell line, suggesting that 65 nt oligos are better recombineering substrates in human cells than are shorter oligos. Although in our previous optimization studies in *E. coli*, little or no additional benefit was added by lengthening oligos beyond 70 nt [15], it remains to be determined if longer oligos could be more efficient for ICP8-stimulated recombineering.

Oligo uptake has been positively correlated with gene targeting frequency [22, 23, 27]. When the effect of oligo concentration on 293T recombineering was evaluated by titrating cells with a 65 nt oligo from 4 to 256 nM (Fig 5 panel B), recombination rates improved as a function of oligo concentration and approached 96% saturation at 50 nM oligo for both endogenous and ICP8-enhanced recombination.

ICP8 requires replicating cells

In the course of these studies, it became evident that some of the fluctuation in recombination rates observed was due to differences in the density of cells plated before addition of oligos. When cell plating density was varied from 5,000 to 50,000 cells/cm2, it was observed that the stimulation in recombination by ICP8 in the presence of 50 nM oligo was only seen at lower cell density (Fig 5 panel C), conditions that promote more replication and consistent with the model that ssDNA recombineering targets replication intermediates (see Strand bias subsection, below).

Strand bias

In bacterial recombineering and in mammalian gene targeting the most efficient substrates are oligos that target the lagging strand template [15, 21, 25]. Since the eGFP^{Y203} transgene was delivered to cells by lentiviral transduction, the reporter target gene was likely integrated in random orientations in individual cells with respect to chromosomally initiated replication forks. Therefore, we predicted that oligos targeting each strand of the Yellow target would produce recombinants at equal frequency when using pools of cells with randomly integrated target genes. Surprisingly, when either DNA strand was targeted in parallel experiments with oligos resembling either the sense or the antisense sequence of the Yellow target, the oligos with the antisense sequence consistently produced more Green cells (Fig 5 panel A). By subtracting the background of endogenous recombination, it became evident that only antisense oligos acted as ICP8-dependent recombineering substrates.

The observed strand bias was not likely due to MMR acting on recombination intermediates differently as the four nucleotide mismatch in heteroduplex recombination intermediates formed when hybridized to the lagging strand template (S2 Fig panel B) are predicted to evade MMR [15] and MMR activity is largely absent in 293T cells [14, 28]. Likewise, the direction of transcription was not likely relevant based on previous studies of strand bias in gene targeting [2, 25]. It was previously seen that replication was essential for gene targeting [29, 30] and that the lagging strand template in DNA synthesis provided the best target for oligo-mediated recombination [2, 15, 21] (Fig 1). Since the Yellow reporter target gene was likely integrated in random orientations in each individual cell with respect to chromosomally initiated replication forks, we cannot account for this bias based on proximity and orientation with respect to endogenous origins of replication. However, the lentiviral vector pDual-Yellow contains an SV40 origin of replication located 5' to the *eGFP*^{Y203} gene (Fig 2 panel A). If this SV40 origin initiated replication with the help of the T antigen expressed in 293T cells, then we expected antisense oligos to hybridize to the lagging strand template and produce the observed recombinants. 293T cell line was created using a temperature sensitive variant of the SV40 T antigen that fails to initiate replication from the SV40 origin at elevated temperature [31]. To determine

if replication from the SV40 origin played a roll, gene targeting was examined at 39.5˚C, a non-permissive temperature for activation of the SV40 origin by T antigen. As seen before, at 37˚C, the strand bias in gene targeting was evident in both the presence and absence of ICP8. However at 39.5˚C, recombination rates were reduced and strand bias eliminated (Fig 6). From this observation we conclude that SV40 origin-dependent replication across the target locus improved gene targeting frequencies and was responsible for the target strand bias.

Discussion

Our observations are consistent with the proposal that ICP8 is a SynExo synaptase subunit like Beta protein from bacteriophage λ. It has been previously demonstrated that Beta protein directs ssDNA recombination substrates to complementary sequences exposed at the replication fork. Our data suggest that T antigen-dependent replication across the target gene stimulates ssDNA recombination by exposing ssDNA primarily on the lagging strand template between Okazaki fragments. Single-strand DNA gaps on the lagging strand template expose complementary sequences to the "antisense" oligos. These results bear striking similarity to bacteriophage SynExo-mediated recombination operating in bacteria. Supporting this conclusion, we found that ICP8 promoted gene targeting only when the cells were seeded at low density and had the opportunity to replicate several times after oligo transfection. The DNA sequence of the recombinant Green fluorescent cells confirmed that genetic information in the oligo was precisely transferred to the target genome by recombineering. We predict that the acquisition of the oligo sequence reflects oligo annealing by ICP8 to the homologous target region accompanied by limited DNA synthesis and ligation to covalently join the introduced oligo to the genome. The details of this mechanism remain to be determined, but as modeled in Fig 1, the oligo sequence once incorporated, could be either repaired by MMR or stably transmitted after a round of DNA synthesis.

Strikingly, the well-studied and commonly used bacteriophage λ synaptase Beta not only failed to stimulate recombination, but significantly inhibited gene targeting by endogenous functions. These results recapitulate recent studies where Beta expression in HT1080 cells did not promote chromosomal gene correction [32]. Instead, the authors demonstrated a modest stimulation of gene editing by Beta using a co-transfected plasmid as the target replicon. When HHV1 infect human cells ICP8 localizes to subnuclear domains called pre-replicative sites [18] and physically associates with several human proteins involved in DNA metabolism and chromatin remodeling [33]. In this study expression of ICP8 independent of the other HHV1 proteins is diffuse in some cells and makes punctate foci in other cells. HumBeta also accumulates in the nucleus, but it does not form the punctate staining foci seen in ICP8 expressing cells (S4 Fig). Images of Beta expression in HT1080 cells also show an enrichment of Beta protein near the nuclear periphery and not in subnuclear punctate foci [32]. Perhaps organization into subnuclear assemblies is required for host-specific protein interactions required to stimulate recombination. HumBeta might lack the ability to synergistically interact with human endogenous functions to promote strand annealing and, instead, sequesters ssDNA substrates from endogenous recombination functions. Given that the degree of stimulation of gene editing by ICP8 in the human genome exceeds that of Beta but is similar to Beta acting on synthetic extrachromosomal DNA targets, we propose that ssDNA annealing proteins have near universal function but must be tuned to the molecular context, *e.g.* genomic chromatin.

These results are consistent with the model that viral synaptase-mediated recombineering is host-specific [4, 34, 35] due to co-evolution of viral SynExo recombinases and host cell proteins. According to this model, recombineering is host-specific because viral SynExo complexes cooperate with cellular functions to promote recombineering and viral development.

We suggest that SynExo interactions with host proteins are required to coordinate recombineering in replication forks. In order to achieve the high rates of recombineering obtained in finely tuned bacterial systems, the human viral SynExo recombination mechanism will likely benefit from coordination with the cell cycle.

We observed an average of ~0.1% oligo-dependent gene targeting in the absence of ICP8, likely facilitated by endogenous cellular recombination functions such as Rad52, a synaptase protein with structure and function similar to viral synaptases [36, 37]. Both endogenous and ICP8-stimulated gene targeting in 293T cells may have benefitted from impaired MMR [28, 38] and increased replication in the presence of the T antigen [39, 40].

While previous data suggest that ICP8 and Rad52 partially overlap in function [14], we found that the human viral synaptase ICP8 significantly (albeit modestly) and reproducibly increased gene targeting rates. Although ICP8 stimulated recombination, we suspect that our results underestimate these rates. ICP8 expression was observed to reduce cell viability (data not shown), likely leading to reduced recovery of recombinants. Indeed, by gating for the remaining ICP8 expressing cells after outgrowth, recombinants were enriched, raising stimulation of ICP8-mediated recombination (from 2.3-fold to 4.7-fold in Fig 3 panels C and D). Future efforts will capitalize on this enrichment method. Addition of a PEST degradation tag to ICP8 should reduce its half-life, possibly improving cell viability. Coupling ICP8 expression to entry into S phase might coordinate production of the bolus of ICP8 with the appearance of Okazaki fragment replication intermediates that increase target site accessibility. Alternatively, ICP8 mRNA and ssDNA oligos could be co-transfected into cell cycle synchronized cells. Another approach that might reduce ICP8 toxicity would be to form ICP8 protein and ssDNA complexes in vitro and deliver them to cells [41, 42].

An alternative strategy might develop the endogenous ssDNA binding protein Rad52 as a recombineering tool. Rad52 appears to have originated from a viral synaptase gene [43] and functionally overlaps with ICP8 in recombinational repair of DNA breaks [14]. Previous studies indicated that Rad52 overexpression might increase gene targeting rates [44, 45, 46] but that sustained high-level expression is detrimental to viability and recovery of recombinants [47], consistent with our observations with constitutively expressed ICP8. We suggest that Rad52 could perform as a recombineering synaptase and is contributing to the endogenous "background" recombination we observed in the absence of ICP8.

Much remains to be learned about the human genome. Development of efficient and specific tools for genome editing is essential to dissect the role of specific alleles on human health and disease. Recombineering optimization in microbes elevated the efficiency from 6% [2] to 15% of total cells, 40% of transfected cells, and 85% of transfected cells that are mismatch repair deficient [15]. Further improvement of eukaryotic cell recombineering might make this a worthy partner to CRISPR/Cas9 as a homologous recombination partner. The twin revolutions of stem cell therapy and genomics are providing the tools for precision medicine and a deeper understanding of human development. Extension of human cell recombineering to stem cell genome editing may lead to development of autologous stem cell genetic therapy and development of better disease models. Our results suggest that ICP8 is a *bona fide* synaptase in the SynExo family of viral two component recombinases [1, 13] and further encourages the development of organism-specific SynExos for genome editing in other species.

Materials and methods

Plasmids

The pDual-eGFP(Y203) lentiviral plasmid was used to create the target for ssDNA oligo-mediated gene targeting, the reporter for recombineering. A scheme for it and the parental plasmid

pDual-eGFP is represented in Fig 2 panel A, while their design and construction were described in [15]. pCMV-ICP8 complements UL29 mutant HHV1 in transfected cells [48] and was used for transient ICP8 transfection and as the source of ICP8 for lentiviral vectors. ICP8 and Beta synaptase genes were individually cloned into the pSLIK-Zeo lentivirus vector for high transduction efficiency, zeocin selection and doxycycline inducibility [49]. The synaptase genes were fused to the E2-Crimson fluorescent protein gene [16] through a P2A linker [17] to follow synaptase expression (S3 Fig). Cloning details are described in Extended Methods.

Oligonucleotides

Oligos were 35 to 65 nt long and complementary to the target region except for a two-nucleotide change specifying Yellow to Green and a silent two-nucleotide substitution at the adjacent serine codon (Figs 2 and S2 panel A). Unmodified ssDNA (oligos) were purchased from Sigma-Aldrich and their sequences are shown in S2 Table.

Cell lines

293T-Yellow recombineering reporter cell lines were created by transducing 293T cells with lentivirus produced from pDual-eGFP(Y203) [15]. Inducible Synaptase-Crimson cell lines were created from 293T-Yellow cells transduced with pSLIK lentiviral clones 1–6. Transduction protocols are described in Extended Methods.

Human cell gene targeting by recombineering

ssDNA recombineering was performed in exponentially growing 293T-Yellow cells expressing a viral synaptase (ICP8 or HumBeta). In experiments in which ICP8 was expressed from a transiently transfected plasmid (as in Figs 3 and 5 panel A and S4 and S5), 293T-Yellow cells were first transfected using 6 μl Fugene 6 (Roche) and 2 μg pCMV-ICP8 per well in 6 well plates in triplicates. In stable 293T- Yellow-pSLIK cell lines encoding ICP8 or HumBeta, cells were first induced with 1 μg/ml doxycycline. The next day, cells were seeded in 24-well plates in 0.5 ml 5% FBS-DMEM at 5,000 cells/cm2. The following day, cells were transfected by mixtures of Lipofectamine 2000 (Invitrogen) and unmodified oligos to a final Lipofectamine concentration of 0.27% and oligo concentration of 50–200 nM as indicated in the figures and text. Cells were passed to 6-well plates and collected for flow cytometry as they reached confluency in the well, usually 13–15 days after transfection, depending on cell recovery after oligo transfection. Fluorescent Green recombinants were distinguished from Yellow parental cells by flow cytometry using narrow bandpass filters (510 ± 15 nm and 540 ± 10 nm) and a differential angular distribution that allowed quantification of each cell without compensation.

Recombination frequencies were calculated as the frequency of Green cells among total (Green + Yellow) fluorescent cells (typically ~50,000 cells per trial).

Additional protocols to be found in S1 Extended Methods.

Disclaimer

The contents do not represent the views of the Department of Veterans Affairs or the United States Government.

Supporting information

S1 Fig. SynExo genes are found in dsDNA viruses that infect Bacteria, Archae and Eukarya. Orthologous protein sequences were detected in sequenced genomes via reiterative use of PSI-BLAST against the non-redundant protein sequence (nr) database with a cut off of 0.005 until

convergence was reached. Query sequences: NP_040616.1 (Lambda exo); NP_059594.1 (phage P22 Abc2); NP_415865.1 (Rac prophage RecE); NP_040617.1 (lambda Beta); NP_415865.1 (Rac prophage RecT); YP_009137104.1 (Human alphaherpesvirus 1 ICP8); NP_613196.1 (*Mamestra configurata* nucleopolyhedrovirus A LEF-3); NP_059596.1 (phage P22 ERF); CAA86623.1 (*Saccharomyces cerevisiae* Rad52). Numbers reflect the number of unique species in which viral SynExo subunit genes were found in integrated viruses in their genomes or in sequenced viruses specific for these organisms. The numbers are color-coded to show the distribution of different SynExo protein families. Examples of some SynExo complexes are listed in S1 Table.
(PDF)

S2 Fig. Recombineering substrates and targets. A) Oligos for fluorescent protein engineering in human cells. Oligos that introduce a change in the target gene were used to evaluate recombineering and oligos that retained the target sequence were used as a "selfing" control. The labels next to the oligos refer to oligo numbers in S2 Table, the amino acid encoded at position 203 in the oligo, the strand identity of the oligo sequence with respect to the direction of transcription across the target gene, and the oligo length in nucleotides. The strand specificity of the oligo is notated as sense "s" or antisense "as" relative to the eGFPY203 coding sequence. B) Mismatches produced in recombination intermediates during annealing of oligo 85 (top) and oligo 84 (bottom) to the complementary strand of the Yellow gene target sequence. The oligos introduce the sequence for threonine at position 203, which changes the fluorescence spectral properties from Yellow to Green. There is a four nucleotide mismatch when targeting the Yellow gene with these oligos.
(PDF)

S3 Fig. Scheme for lentiviral plasmids encoding doxycycline-inducible synaptases. Synaptase genes were fused to a red fluorescent gene, E2-Crimson (Strack et al. 2009) through a P2A linker (Szymczak-Workman et al. 2012) in a single open reading frame. The P2A linker causes ribosome skipping to produce equimolar amounts of the upstream and downstream protein products. The P2A peptide leaves a proline residue at the N-terminal end (Nt) of the C-terminal (Ct) protein and an 18 amino acid peptide at the Ct of the Nt protein. Previous reports have shown that these synaptases are moderately defective when fused to reporter genes (Taylor et al. 2003; Poteete 2011). Since we didn't know if any of these additions might affect the recombination activity of the proteins, E2-Crimson was cloned either upstream or downstream of the synaptases in separate lentiviral constructs.
(PDF)

S4 Fig. ICP8 and HumBeta synaptases localize to the nucleus. Expression of viral synaptases and the Crimson reporter from pSLIK plasmids was validated in 293T cells. 293T cells were transiently transfected with each pSLIK plasmid and synaptase expression was induced with 1 μg/ml doxycycline in the media for 48 hours. ICP8 and HumBeta were detected by immunocytochemistry using anti-ICP8 (Abcam, ab20193) and anti-HA antibodies (Abcam, ab9110), respectively. Briefly, 293T cells were seeded onto poly-L-Lysine (Sigma) coated coverslips in 6 well plates in media. When cells were ready for imaging, cells adhering to coverslips were washed 3 times with PBS and then fixed in 4% paraformaldehyde in PBS pH 7.4 for 15 min at room temperature. Cells were washed 3 times with PBS and permeabilized with 0.25% Triton X-100 for 10 min. Cells were washed again and blocked with 1% BSA, 0.3 M glycine in PBST for 30 min. Cells were incubated with the primary antibody in 1% BSA in PBST in a humidified chamber overnight at 4˚C. Cells were washed 3 times with PBS and incubated with the secondary antibody (which were labeled by Alexa Fluor) in 1% BSA for 1 hour at room temperature in the dark. Cells were washed and incubated with 0.5 μg/ml DAPI for 10 min. Cells

were washed, mounted with Prolong antifade or Vectashield (Vector Laboratories). Cells were viewed with a Nikon Diaphot equipped with a Retiga 1300 camera. A Nikon 20X objective was used. Images were collected and analysed using IP-Lab software package. ICP8 and HumBeta are coloured green, E2-Crimson is coloured Red and DAPI is coloured blue.
(PDF)

S5 Fig. ICP8 and HumBeta expression from pSLIK plasmids in transiently transfected 293T cells. 293T cells transfected with lentiviral vectors in the presence and absence of doxycycline (1 μg/ml) were collected 24 hours after transfection and analysed by Western blot as described by Abcam. ICP8 was detected with primary Herpes Virus I ICP8 Major DNA Binding Protein antibody (Abcam, ab20193) mouse monoclonal IGg1 and goat anti-mouse IGg1 secondary HRP labelled antibody [sc-2064] (Santa Cruz). HumBeta was detected with primary rabbit polyclonal anti-HA antibody (Abcam, ab9110) and goat anti-rabbit IgG secondary HRP labelled antibody [sc-2064] (Santa Cruz). Membranes were washed three times in TBST and incubated with the ECL Plus Western Blotting Detection System (from GE Healthcare RPN2132) for 5 min or until the bands glowed visibly. Films were exposed to membranes for varying amounts of time and then developed. Films were scanned and analysed using Photoshop or Image J software. A) ICP8 expression from pSLIK1 and pSLIK4 co-migrates with ICP8 expressed from the pCMV-ICP8 control. B) HumBeta expression from pSLIK2 and pSLIK5. The table indicates the masses of predicted protein products and observed outcomes in these Western Blots. All fusion proteins demonstrated >99% ribosome skipping efficiency, separating reporter fluorescent proteins from synaptases (trace amounts of fusion proteins were only evident when films were greatly overexposed, data not shown).
(PDF)

S6 Fig. Gene targeting is stimulated by HHV1 ICP8 and inhibited by phage λ Beta in human cells. This figure includes recombineering data from all pSLIK cell lines. Recombineering reporter cell lines 293T-Yellow-pSLIK cells were incubated with 1 μg/ml doxycycline to induce synaptase expression and seeded in 24 well plates at 5,000 cells/cm2. The next day, cells were transfected with 50 nM of oligo 85. Fluorescent cells were quantified by flow cytometry and recombination efficiency was calculated by dividing the number of Green cells by the total number of fluorescent cells counted (typically ~50,000 cells per trial). The background of green cells in "no oligo" control experiments (never exceeding 0.02%) was subtracted from recombination frequencies and plotted. Data were evaluated by Fisher's Exact Test of significance; *** indicates $P<0.005$ and **** indicates $P<0.001$. n = 3 and error bars reflect SEM.
(PDF)

S7 Fig. Recombinant green genotype detection by allele-specific PCR. Recombinant green fluorescent cells from experiment 82 in Fig 2F were enriched by cell sorting. Genomic DNA was isolated and the target gene was amplified by PCR using Taq 2X Master Mix (NEB). For each allele-specific PCR reaction, one of the primers in the pair was complementary at the 3' end to the template sequence of one of two compared alleles, to specifically amplify that allele sequence. As a control, the same primer pair was used with the other allele's template. Green primers correspond to oligos 45 and 75 and Yellow primers correspond to oligos 45 and 74. The annealing temperature was optimized to 70.8˚C to make amplification selective for each sequence. Reactions were performed as recommended (NEB). Allele-specific PCR shows evidence of genuine Green recombinant allele sequences among non-recombinant Yellow genes in a mixed population. Experimental details for this experiment can be found in S1 Extended Methods under "Determination of recombinant genotype".
(PDF)

S1 Table. Examples of SynExo functional modules.
(PDF)

S2 Table. Oligonucleotides used in this study.
(PDF)

S1 Additional References.
(PDF)

S1 Extended Methods.
(PDF)

S1 Data.
(XLSX)

S1 DNA Sequences.
(PDF)

Acknowledgments

The authors thank Dr. David Knipe for the plasmid pCMV-ICP8, Dr. Jakob Reiser for the plasmid pENTR2B/TREPitt and for advice about lentivirus engineering, Dr. Priya Rai for the 293T cells and lentiviral plasmids pHR' CMV 8.2ΔR and pCMV-VSV-G, Dr. Adriana Gomez for her help with microscopy, Dr. Kate M. Vignali and Dr. Dario A. A. Vignali for advice with the 2A peptide constructs, and Drs. Guy Howard, Carlos Perez-Stable, and Ramiro Verdun for critically reading the manuscript. This work was supported by the National Institutes of Health [F31-GM089125-01] to MV, funds from the University of Miami Department of Biochemistry and Molecular Biology to RSM, Department of Veterans Affairs, Veterans Health Administration, Office of Research and Development (Biomedical Laboratory Research and Development) Merit Review award [BX000952] to PSC and funds from the Miami VA Geriatric Research, Education, and Clinical Center to PSC and MVC.

Author Contributions

Conceptualization: Melvys Valledor, Richard S. Myers, Paul C. Schiller.

Data curation: Melvys Valledor, Richard S. Myers.

Formal analysis: Melvys Valledor, Richard S. Myers.

Funding acquisition: Melvys Valledor, Richard S. Myers, Paul C. Schiller.

Investigation: Melvys Valledor, Richard S. Myers, Paul C. Schiller.

Methodology: Melvys Valledor, Richard S. Myers, Paul C. Schiller.

Project administration: Richard S. Myers, Paul C. Schiller.

Resources: Richard S. Myers, Paul C. Schiller.

Supervision: Richard S. Myers, Paul C. Schiller.

Validation: Richard S. Myers.

Writing – original draft: Melvys Valledor, Richard S. Myers, Paul C. Schiller.

Writing – review & editing: Melvys Valledor, Richard S. Myers, Paul C. Schiller.

References

1. Vellani TS, Myers RS. Bacteriophage SPP1 Chu is an alkaline exonuclease in the SynExo family of viral two-component recombinases. J Bacteriol. 2003 Apr; 185(8):2465–74. https://doi.org/10.1128/JB.185.8.2465-2474.2003 PMID: 12670970
2. Ellis HM, Yu D, DiTizio T, Court DL. High efficiency mutagenesis, repair, and engineering of chromosomal DNA using single-stranded oligonucleotides. Proc Natl Acad Sci U S A. 2001 Jun 5; 98 (12):6742–6. https://doi.org/10.1073/pnas.121164898 PMID: 11381128
3. Zhang Y, Muyrers JP, Rientjes J, Stewart AF. Phage annealing proteins promote oligonucleotide-directed mutagenesis in Escherichia coli and mouse ES cells. BMC Mol Biol. 2003 Jan 16; 4(1):1. https://doi.org/10.1186/1471-2199-4-1 PMID: 12530927
4. Murphy KC. Phage recombinases and their applications. Adv Virus Res. 2012; 83:367–414. https://doi.org/10.1016/B978-0-12-394438-2.00008-6 PMID: 22748814
5. Datta S, Costantino N, Zhou X, Court DL. Identification and analysis of recombineering functions from Gram-negative and Gram-positive bacteria and their phages. Proc Natl Acad Sci U S A. 2008 Feb 5; 105(5):1626–31. https://doi.org/10.1073/pnas.0709089105 PMID: 18230724
6. van Kessel JC, Hatfull GF. Efficient point mutagenesis in mycobacteria using single-stranded DNA recombineering: characterization of antimycobacterial drug targets. Mol Microbiol. 2008 Mar; 67 (5):1094–107. https://doi.org/10.1111/j.1365-2958.2008.06109.x PMID: 18221264
7. Dekker M, Brouwers C, Aarts M, van der Torre J, de Vries S, van de Vrugt H et al. Effective oligonucleotide-mediated gene disruption in ES cells lacking the mismatch repair protein MSH3. Gene Ther. 2006 Apr; 13(8):686–94. https://doi.org/10.1038/sj.gt.3302689 PMID: 16437133
8. Myers RS, Rudd KE. Mining DNA sequences for molecular enzymology: The Red alpha superfamily defines a set of recombination nucleases, Miami Nature Biotech Nucleic Acids Symp Ser. 1998; (38):49–50.
9. Aravind L, Makarova KS, Koonin EV. SURVEY AND SUMMARY: holliday junction resolvases and related nucleases: identification of new families, phyletic distribution and evolutionary trajectories. Nucleic Acids Res. 2000 Sep 15; 28(18):3417–32. PMID: 10982859
10. van Kessel JC, Hatfull GF. Recombineering in Mycobacterium tuberculosis. Nat Methods. 2007 Feb; 4 (2):147–52. https://doi.org/10.1038/nmeth996 PMID: 17179933
11. van Pijkeren JP, Britton RA. High efficiency recombineering in lactic acid bacteria. Nucleic Acids Res. 2012 May; 40(10):e76. https://doi.org/10.1093/nar/gks147 PMID: 22328729
12. Swingle B, Markel E, Costantino N, Bubunenko MG, Cartinhour S, Court DL. Oligonucleotide recombination in Gram-negative bacteria. Mol Microbiol. 2010 Jan; 75(1):138–48. https://doi.org/10.1111/j.1365-2958.2009.06976.x PMID: 19943907
13. Reuven NB, Staire AE, Myers RS, Weller SK. The herpes simplex virus type 1 alkaline nuclease and single-stranded DNA binding protein mediate strand exchange in vitro. J Virol. 2003 Jul; 77(13):7425–33. https://doi.org/10.1128/JVI.77.13.7425-7433.2003 PMID: 12805441
14. Schumacher AJ, Mohni KN, Kan Y, Hendrickson EA, Stark JM, Weller SK. The HSV-1 exonuclease, UL12, stimulates recombination by a single strand annealing mechanism. PLoS Pathog. 2012; 8(8): e1002862. https://doi.org/10.1371/journal.ppat.1002862 PMID: 22912580
15. Valledor M, Hu Q, Schiller P, Myers RS. Fluorescent protein engineering by in vivo site-directed mutagenesis. IUBMB Life. 2012 Aug; 64(8):684–9. https://doi.org/10.1002/iub.1041 PMID: 22639380
16. Strack RL, Hein B, Bhattacharyya D, Hell SW, Keenan RJ, Glick BS. A rapidly maturing far-red derivative of DsRed-Express2 for whole-cell labeling. Biochemistry. 2009 Sep 8; 48(35):8279–81. https://doi.org/10.1021/bi900870u PMID: 19658435
17. Szymczak-Workman AL, Vignali KM, Vignali DA. Design and construction of 2A peptide-linked multicistronic vectors. Cold Spring Harb Protoc. 2012 Feb 1; 2012(2):199–204. https://doi.org/10.1101/pdb.ip067876 PMID: 22301656
18. Taylor TJ, McNamee EE, Day C, Knipe DM. Herpes simplex virus replication compartments can form by coalescence of smaller compartments. Virology. 2003 May 10; 309(2):232–47. PMID: 12758171
19. Poteete AR. Recombination phenotypes of Escherichia coli greA mutants. BMC Mol Biol. 2011 Mar 31; 12:12. https://doi.org/10.1186/1471-2199-12-12 PMID: 21453489
20. de Bruyn Kops A, Knipe DM. Formation of DNA replication structures in herpes virus-infected cells requires a viral DNA binding protein. Cell. 1988 Dec 2; 55(5):857–68. PMID: 2847874
21. Li XT, Costantino N, Lu LY, Liu DP, Watt RM, Cheah KS et al. Identification of factors influencing strand bias in oligonucleotide-mediated recombination in Escherichia coli. Nucleic Acids Res. 2003 Nov 15; 31 (22):6674–87. https://doi.org/10.1093/nar/gkg844 PMID: 14602928

22. Nickerson HD, Colledge WH. A comparison of gene repair strategies in cell culture using a lacZ reporter system. Gene Ther. 2003 Sep; 10(18):1584–91. https://doi.org/10.1038/sj.gt.3302049 PMID: 12907950

23. Andrieu-Soler C, Casas M, Faussat AM, Gandolphe C, Doat M, Tempé D et al. Stable transmission of targeted gene modification using single-stranded oligonucleotides with flanking LNAs. Nucleic Acids Res. 2005 Jul 7; 33(12):3733–42. https://doi.org/10.1093/nar/gki686 PMID: 16002788

24. Rios X, Briggs AW, Christodoulou D, Gorham JM, Seidman JG, Church GM. Stable gene targeting in human cells using single-strand oligonucleotides with modified bases. PLoS One. 2012; 7(5):e36697. https://doi.org/10.1371/journal.pone.0036697 PMID: 22615794

25. Aarts M, te Riele H. Parameters of oligonucleotide-mediated gene modification in mouse ES cells. J Cell Mol Med. 2010 Jun; 14(6B):1657–67. https://doi.org/10.1111/j.1582-4934.2009.00847.x PMID: 19627401

26. Gourves AS, Tanguy Le Gac N, Villani G, Boehmer PE, Johnson NP. Equilibrium binding of single-stranded DNA with herpes simplex virus type I-coded single-stranded DNA-binding protein, ICP8. J Biol Chem. 2000 Apr 14; 275(15):10864–9. PMID: 10753882

27. Aarts M, te Riele H. Subtle gene modification in mouse ES cells: evidence for incorporation of unmodified oligonucleotides without induction of DNA damage. Nucleic Acids Res. 2010 Nov; 38(20):6956–67. https://doi.org/10.1093/nar/gkq589 PMID: 20601408

28. Trojan J, Zeuzem S, Randolph A, Hemmerle C, Brieger A, Raedle J et al. Functional analysis of hMLH1 variants and HNPCC-related mutations using a human expression system. Gastroenterology. 2002 Jan; 122(1):211–9. PMID: 11781295

29. Olsen PA, Randøl M, Luna L, Brown T, Krauss S. Genomic sequence correction by single-stranded DNA oligonucleotides: role of DNA synthesis and chemical modifications of the oligonucleotide ends. J Gene Med. 2005 Dec; 7(12):1534–44. https://doi.org/10.1002/jgm.804 PMID: 16025558

30. Poteete AR. Involvement of Escherichia coli DNA Replication Proteins in Phage Lambda Red-Mediated Homologous Recombination. PLoS One. 2013 Jun 19; 8(6):e67440. https://doi.org/10.1371/journal.pone.0067440 PMID: 23840702

31. Rio DC, Clark SG, Tjian R. A mammalian host-vector system that regulates expression and amplification of transfected genes by temperature induction. Science. 1985 Jan 4; 227(4682):23–8. PMID: 2981116

32. Xu K, Stewart AF, Porter AC. Stimulation of oligonucleotide-directed gene correction by Redβ expression and MSH2 depletion in human HT1080 cells. Mol Cells. 2015 Jan 31; 38(1):33–9. https://doi.org/10.14348/molcells.2015.2163 PMID: 25431426

33. Taylor TJ, Knipe DM. Proteomics of herpes simplex virus replication compartments: association of cellular DNA replication, repair, recombination, and chromatin remodeling proteins with ICP8. J Virol. 2004 Jun; 78(11):5856–66. https://doi.org/10.1128/JVI.78.11.5856-5866.2004 PMID: 15140983

34. Thomason L, Costantino N, Sawitzke J, Datta S, Bubunenko M, Court D et al. 2005. Recombineering in Prokaryotes, p 383–399. *In* Waldor M, Friedman D, Adhya S (ed), *Phages*. ASM Press, Washington, DC. https://doi.org/10.1128/9781555816506.ch19

35. van Kessel JC, Marinelli LJ, Hatfull GF. Recombineering mycobacteria and their phages. Nat Rev Microbiol. 2008 Nov; 6(11):851–7. https://doi.org/10.1038/nrmicro2014 PMID: 18923412

36. Shinohara A, Shinohara M, Ohta T, Matsuda S, Ogawa T. Rad52 forms ring structures and co-operates with RPA in single-strand DNA annealing. Genes Cells. 1998 Mar; 3(3):145–56. PMID: 9619627

37. Lopes A, Amarir-Bouhram J, Faure G, Petit MA, Guerois R. Detection of novel recombinases in bacteriophage genomes unveils Rad52, Rad51 and Gp2.5 remote homologs. Nucleic Acids Res. 2010 Jul; 38(12):3952–62. https://doi.org/10.1093/nar/gkq096 PMID: 20194117

38. Cannavo E, Gerrits B, Marra G, Schlapbach R, Jiricny J. Characterization of the interactome of the human MutL homologues MLH1, PMS1, and PMS2. J Biol Chem. 2007 Feb 2; 282(5):2976–86. https://doi.org/10.1074/jbc.M609989200 PMID: 17148452

39. Friedrich TD, Laffin J, Lehman JM. Simian virus 40 large T-antigen function is required for induction of tetraploid DNA content during lytic infection. J Virol. 1992 Jul; 66(7):4576–9. PMID: 1318419

40. Perry MB, Lehman JM. Activities of SV40 T antigen necessary for the induction of tetraploid DNA content in permissive CV-1 cells. Cytometry. 1998 Apr 1; 31(4):251–9. PMID: 9551600

41. Wang Q, Yu J, Kadungure T, Beyene J, Zhang H, Lu Q. ARMMs as a versatile platform for intracellular delivery of macromolecules. Nat Commun. 2018 Mar 6; 9(1):960. https://doi.org/10.1038/s41467-018-03390-x PMID: 29511190

42. DeWitt MA, Corn JE, Carroll D. Genome editing via delivery of Cas9 ribonucleoprotein. Methods. 2017 May 15; 121–122:9–15. https://doi.org/10.1016/j.ymeth.2017.04.003 PMID: 28410976

43. Ploquin M, Bransi A, Paquet ER, Stasiak AZ, Stasiak A, Yu X et al. Functional and structural basis for a bacteriophage homolog of human RAD52. Curr Biol. 2008 Aug 5; 18(15):1142–6. https://doi.org/10.1016/j.cub.2008.06.071 PMID: 18656357

44. Kalvala A, Rainaldi G, Di Primio C, Liverani V, Falaschi A, Galli A. Enhancement of gene targeting in human cells by intranuclear permeation of the Saccharomyces cerevisiae Rad52 protein. Nucleic Acids Res. 2010 Aug; 38(14):e149. https://doi.org/10.1093/nar/gkq486 PMID: 20519199

45. Di Primio C, Galli A, Cervelli T, Zoppè M, Rainaldi G. Potentiation of gene targeting in human cells by expression of Saccharomyces cerevisiae Rad52. Nucleic Acids Res. 2005 Aug 16; 33(14):4639–48. https://doi.org/10.1093/nar/gki778 PMID: 16106043

46. Takahashi N, Dawid IB. Characterization of zebrafish Rad52 and replication protein A for oligonucleotide-mediated mutagenesis. Nucleic Acids Res. 2005 Aug 1; 33(13):e120. https://doi.org/10.1093/nar/gni122 PMID: 16061934

47. Yáñez RJ, Porter AC. Differential effects of Rad52p overexpression on gene targeting and extrachromosomal homologous recombination in a human cell line. Nucleic Acids Res. 2002 Feb 1; 30(3):740–8. PMID: 11809887

48. Taylor TJ, Knipe DM. C-terminal region of herpes simplex virus ICP8 protein needed for intranuclear localization. Virology. 2003 May 10; 309(2):219–31. PMID: 12758170

49. Shin KJ, Wall EA, Zavzavadjian JR, Santat LA, Liu J, Hwang JI et al. A single lentiviral vector platform for microRNA-based conditional RNA interference and coordinated transgene expression. Proc Natl Acad Sci U S A. 2006 Sep 12; 103(37):13759–64. https://doi.org/10.1073/pnas.0606179103 PMID: 16945906